Available online at www.sciencedirect.com
SCIENCE DIRECT
Polymer 46 (2005) 8313–8320
polymer
www.elsevier.com/locate/polymer

Development of co-continuous structure in liquid crystalline polyester

Kenta Suzuki[a], Hiromu Saito[a,*], Masatoshi Tokita[b], Junji Watanabe[b]

[a]*Department of Organic and Polymer Materials Chemistry, Tokyo University of Agriculture and Technology, Nakacho, Koganei-shi, Tokyo 184-8588, Japan*
[b]*Department of Organic and Polymeric Materials, Tokyo Institute of Technology, Ookayama, Meguro-ku, Tokyo 152-8552, Japan*

Received 14 December 2004; received in revised form 7 June 2005; accepted 14 June 2005
Available online 20 July 2005

Abstract

We investigated liquid crystallization of liquid crystalline polyester BB-5 during isothermal annealing by digital high-fidelity microscope and light scattering. A liquid crystalline spherical domain having a radius of micrometers appeared by annealing at around 180 °C. The domain grew dendritically in all directions. Neighboring liquid crystalline regions coalesced and then interconnected. The interconnected structure changed to a co-continuous two-phase structure with increasing ordering of the liquid crystalline phase, and the interface between the liquid crystalline phase and the isotropic phase became smoother over time. Liquid crystallization stopped before volume filling the whole space, and the liquid crystalline phase and isotropic phase coexisted. The liquid crystalline region became narrower with an increase in the temperature of the liquid crystallization. Such structural development is different from the liquid–liquid phase separation via spinodal decomposition, and it may be attributed to the segregation of non-liquid crystallizable low molecular weight molecules from the growth front by fractionation of the molecular weight distribution during the liquid crystallization in terms of the instability of the diffusion-controlled interface.

Keywords: Liquid crystalline polyester; Morphology development; Fractionation

1. Introduction

The increase of density fluctuations during the induction period prior to crystallization of crystalline polymers has been proposed as the result of small angle X-ray scattering (SAXS) and wide angle X-ray scattering (WAXS). The SAXS peak corresponding to density fluctuation having a wavelength of several tens of nanometers increases exponentially with time before the appearance of the Bragg peak in WAXS. This increase suggests that liquid–liquid phase separation via spinodal decomposition occurs during the induction period of the crystallization. Such spinodal decomposition has been reported in poly(ethylene terephthalate) (PET) [1,2], poly(ether ketone ketone) [3], isotactic polypropylene [4,5], and isotactic polystyrene [6]. Spinodal decomposition is explained by the kinetic theory of the isotropic-to-nematic transition of polymer liquid crystals; i.e. phase separation is induced by the parallel orientational ordering of rigid polymer segments prior to crystallization [7,8].

Recently, Wang et al. found a co-continuous structure of a liquid crystalline phase and an isotropic phase having a size of 10 μm in liquid crystalline co-polyester consisting of *p*-hydroxybenzoic acid and ethylene terephthalate [9]. The development of the co-continuous structure was explained by the liquid–liquid phase separation via late stage of the spinodal decomposition. Independently, we found a co-continuous structure consisting of a liquid crystalline phase and an isotropic phase by a drop in temperature from the isotropic melting state to the liquid crystalline state in poly(pentamethylene-4,4′-bibenzoate) (BB-5), which has a structure similar to that of PET and a segmental rigidity higher than that of PET [10]. The liquid crystallization stopped before volume filling of the whole space, and the isotropic melt region remained in spite of the long annealing time.

This paper reports on our investigation of the structural development of BB-5 to help in understanding the origin of the co-continuous structure of BB-5. The investigation was performed by using a digital high fidelity microscope, a polarized optical microscope, and light scattering. The

* Corresponding author. Tel./fax: +81 42 388 7294.
E-mail address: hsaitou@cc.tuat.ac.jp (H. Saito).

0032-3861/$ - see front matter © 2005 Elsevier Ltd. All rights reserved.
doi:10.1016/j.polymer.2005.06.044

results led us to understand that the co-continuous structure is not ascribed to spinodal decomposition but to the segregation of low molecular weight molecules from the growth front of the liquid crystalline phase by the fractionation of the molecular weight distribution. Development of the co-continuous structure is discussed in terms of the instability of the diffusion-controlled interface [11–17].

2. Experimental

This study used the liquid crystalline polyester, BB-5. The BB-5 was synthesized by melt transesterification of dimethyl 4,4′-bibenzoate and pentandiol including five methylenes with isopropyl titanate as a catalyst [18–20].

Table 1 lists the characteristics of BB-5. BB-5(WD) is BB-5 with a wide molecular weight distribution while BB-5(ND) is BB-5 with a narrow molecular weight distribution. The weight average molecular weight M_w, number average molecular weight M_n, and molecular weight distribution M_w/M_n were determined by gel permeation chromatography (GPC) based on data for polystyrene. The isotropization temperature of the smectic phase, T_i, indicating the smectic–isotropic phase transition temperature, was obtained from the exothermic peak in the DSC heating curve. T_i is below the thermal decomposition temperature, and the development of liquid crystallization after the temperature drop from the isotropic melting state can be observed [21,22].

A thin film of ca. 30 μm thick was prepared by melting the pellets at 235 °C for 5 min on a hot stage and pressing them between two cover glasses. The melt specimen at the isotropic melt state was then rapidly quenched to the desired liquid crystallization temperature, T_{lc}. Structural development during isothermal annealing at T_{lc} was observed under a polarized optical microscope (Olympus, BX-50) with a sensitive tint plate and high-fidelity digital microscope (Hirox, MX-50305ZΠ).

Real-time analysis of the isothermal liquid crystallization was performed by the light scattering method. A film specimen on a cover glass was melted at 235 °C for 5 min on a hot stage. The film specimen was then immediately transferred to another hot stage on the light scattering stage and annealed at T_{lc}. A polarized He–Ne laser with a wavelength of 632.8 nm was applied vertically to the film specimen. The scattered light was passed through an analyzer and then onto a highly sensitive charge-coupled device (CCD) camera with a 13.3×8.8 mm^2 sensor having 512×512 pixels (Princeton Instruments, Inc., TE/CDD-512-TKM-1). We employed Hv geometry in which the optical axis of the analyzer was set perpendicularly to that of the polarizer. This enables a time-resolved, one-dimensional measurement with 512 data points in a time scale of 0.2 s. The input data from the CCD camera was digitized by the ST-13X controller. The digitized data were stored in a personal computer for further analysis [23].

Table 1
Characterization of BB-5

Polymer	M_n	M_w	M_w/M_n	T_m (°C)
BB-5(WD)	3472	9819	2.83	190
BB-5(ND)	22,101	42,080	1.90	210

WD, wide molecular weight distribution; ND, narrow molecular weight distribution.

3. Results and discussion

Fig. 1 is a polarized optical micrograph of BB-5(WD) annealed at 180 °C for 1 h. The liquid crystalline texture of the smectic phase having a strong birefringence is seen in this temperature range [18–20]. The noteworthy result here is that a co-continuous structure consisting of a liquid crystalline phase and an isotropic phase was obtained. Another interesting result is that the liquid crystallization stopped before volume filling of the whole space and the isotropic melt region remained in spite of the long annealing period. The stopping of the liquid crystallization with a co-continuous structure is rare in neat polymers, and the co-continuous structure is different from the characteristic liquid crystalline textures such as Schlieren and focal conic textures caused by defects [24–29].

There are two possibilities for the stopping of the liquid crystallization with a co-continuous structure. One is the liquid–liquid phase separation via spinodal decomposition [9] caused by parallel orientational ordering of rigid segments prior to crystallization demonstrated in PET since the segmental rigidity of BB-5 is higher than that of PET [1,2]. The other is the segregation of non-liquid crystallizable low molecular weight molecules from the growth front of the liquid crystalline phase during liquid crystallization by the fractionation of the molecular weight distribution [30,31]. To understand this unique behavior, the

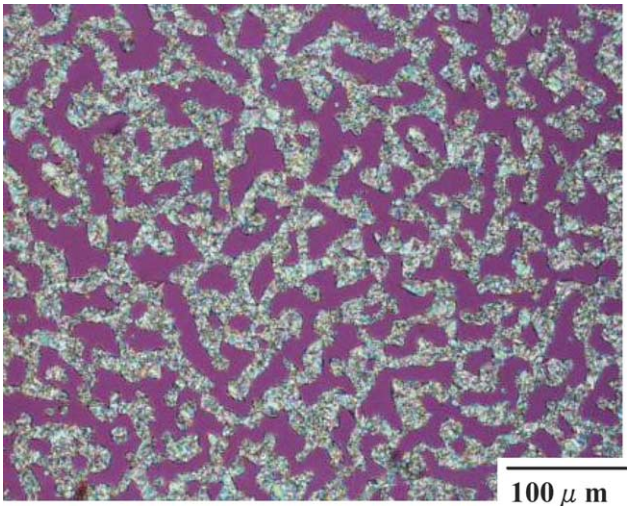

Fig. 1. Polarized micrograph of BB-5(WD) annealed at 180 °C.

morphology development is discussed in the following paragraphs.

Fig. 2 shows the development of the liquid crystalline morphology of BB-5 during isothermal annealing at 180 °C. Initially, spherical domains having a size of several micrometers were detected (Fig. 2(a)). When the domains grew to a size of about 10 μm, protuberances having a width of several micrometers appeared on the surface of the spherical domains (Fig. 2(b)). The spherical domains grew asymmetrically and their shape became distorted, although the protuberances did not propagate into long projections (Fig. 2(c)).

The distorted domains became larger over time and the neighboring domains impinged on each other. The impinged domains coalesced and the interfaces between the domains disappeared (Fig. 2(d)). Because of their coalescence, the distorted domains changed to large branched domains having a size of about 100 μm. The branched domains became larger over time by impinging on and coalescing with the neighboring domains.

After the domains coalesced, the branched and distorted domains changed their shape to long and curved one over time, creating continuously connected domains (Fig. 2(e)). The growth of the liquid crystalline domains stopped before filling the whole space and the interstices between the branches remained as isotropic melt regions. After growth stopped, the optical anisotropy of the continuously connected liquid crystalline phase increased while maintaining the co-continuous structure. The interfaces of the domains became smoother over time, i.e. the branching and distortion of the domains decreased over time (Fig. 2(f)). Finally, a co-continuous structure consisting of a liquid crystalline phase and an isotropic phase shown in Fig. 1 was obtained.

As explained above, the spherical liquid crystalline domains changed into a co-continuous structure through

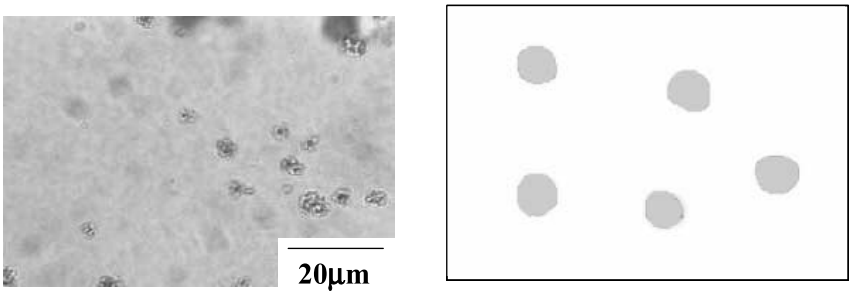

(a) 4 s

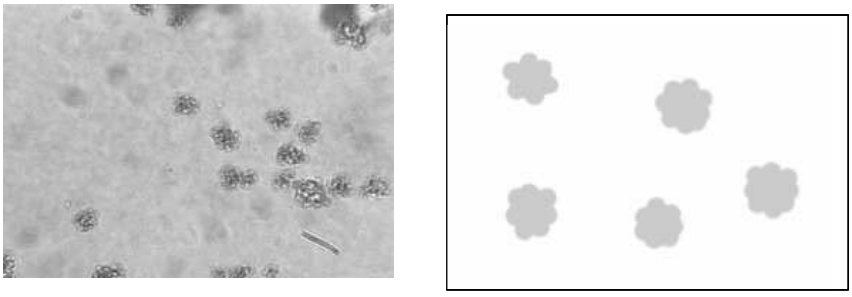

(b) 5 s

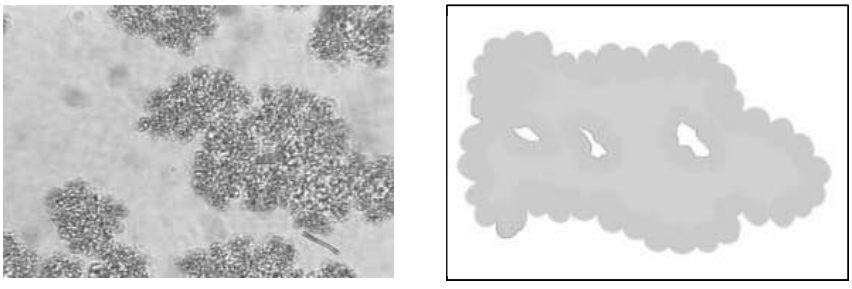

(c) 10 s

Fig. 2. In situ observation of BB-5(WD) during liquid crystallization at 195 °C. Left, digital high-fidelity micrographs; right, schematics.

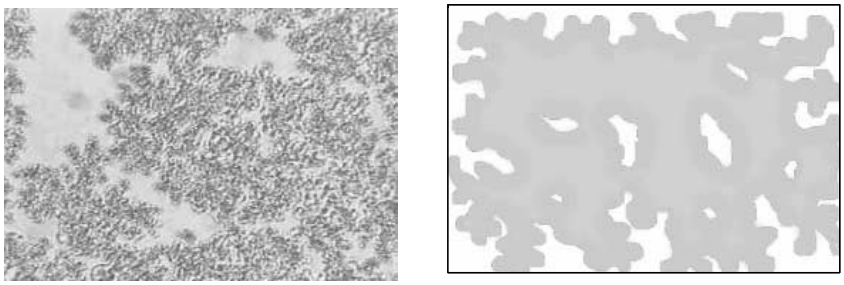

(d) 15 s

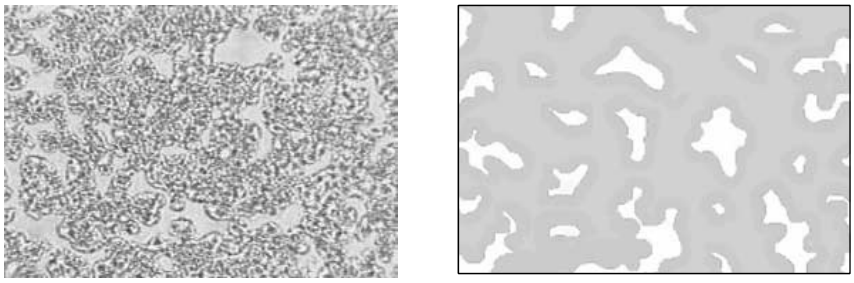

(e) 20 s

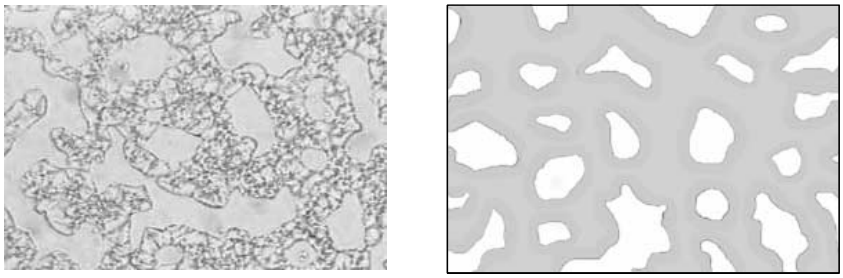

(f) 40 s

Fig. 2 (*continued*)

various stages. This change is quite different from the development of the morphology by liquid–liquid phase separation via spinodal decomposition. The co-continuous structure is usually obtained by spinodal decomposition, though the development of the co-continuous structure in the liquid crystalline co-polyester is explained by the late stage of the spinodal decomposition [10]. Such evolution might be explained by the fractionation of high and low molecular weight molecules during liquid crystallization due to molecular weight distribution, as explained in the following paragraphs.

BB-5(WD) has a wide molecular weight distribution of $M_w/M_n = 2.83$, indicating that it consists of a wide range of different molecular weights. The smectic–isotropic phase transition temperature, T_i, increases with an increase in the molecular weight, as suggested in Table 1. That is, T_i of the higher molecular weight polymer BB-5(ND) is higher than that of the lower molecular weight polymer BB-5(WD). Hence, high molecular weight molecules in BB-5 are liquid crystallizable while low molecular weight molecules are not liquid crystallizable if BB-5 is annealed at a temperature close to T_{lc} after the temperature drop from the isotropic melt state. Non-liquid crystallizable low molecular weight molecules diffuse away from the growth front of the liquid crystalline phase by fractionation during the liquid crystallization of the high molecular weight molecules.

Because of the segregation of the non-liquid crystallizable low molecular weight molecules, a concentration gradient is formed in the isotropic melt region at around the interface between liquid crystalline phase and isotropic phase (Fig. 3(a)) [12]. If part of the flat interface grows faster than another part by some fluctuation, the advanced part can grow faster due to the concentration gradient (Fig. 3(b)). This might induce growth of the protuberances on the surface of the spherical liquid crystalline domains, as shown in Fig. 2(b). According to the Mullins–Sekerka

theory [11,14,16], the stability of the interface is described by

$$\dot{\delta}_{lm} = (l-1) \times \frac{D_c}{c_0 R^2}\left\{(c_\infty - c_e) - (l^2+3l+4)\frac{c_e \Gamma_c}{R}\right\}\delta_{lm} \equiv \omega_{lm}\delta_{im} \quad (1)$$

$$\Gamma_c = \frac{\gamma \omega_0}{k_B T} \quad (2)$$

where δ_{lm} is the deformation amplitude, D_c is the diffusion coefficient, c_0 is the concentration in the liquid crystal, c_∞ is the concentration at infinity, c_e is the equilibrium concentration at the flat interface, R is the radius of spherulite, l is the order of spherical harmonics, Γ_c is the capillary length, γ is the interfacial tension, ω_0 is the atomic volume, k_B is Bolzmann's constant, and T is the absolute temperature. Interfacial stability is determined by the increase and decrease of the deformation amplitude $\dot{\delta}_{lm}$ in Eq. (1). In the { } of Eq. (1), the left term $(c_\infty - c_e)$ is the supersaturation and the right term $(l^2+3l+4)c_e\Gamma_c/R$ is the contribution of the interfacial tension. The supersaturation enhances the perturbation of the interface while the interfacial tension suppresses the perturbation. When the contribution of the supersaturation on $\dot{\delta}_{lm}$ is larger than that of the interfacial tension ($\omega_{lm}>0$), the interface is unstable due to the growth of the deformation, and the protuberances propagate to fibrillar projections and proliferate by divergence of the protuberances. In contrast, when the contribution of the interfacial tension is larger than that of the supersaturation ($\omega_{lm}<0$), deformation decays and the protuberances do not propagate to projections. Thus, the small protuberances in Fig. 2(c) are ascribed to strong interfacial tension.

The spherical domains with small protuberances grew to distorted domains due to the presence of the non-liquid crystallizable low molecular weight molecules at around the growth front of the liquid crystalline phase. That is, the growth rate changes with the concentration of the segregated non-liquid crystallizable molecules at the growth front. Since the liquid crystalline phase is not solidified but is movable, the neighboring domains can coalesce and the interface between each domain disappears when they impinge, as shown in Fig. 2(d). Because of the coalescence, distorted domains change their shape to branched and continuous connected ones. The branched and continuously connected domains are not volume filled and the isotropic melt region remains in the interstices within the branches. The isotropic melt region remains in spite of the long annealing time due to the presence of the non-liquid crystallizable low molecular weight molecules segregated from the growth front.

After the growth of the liquid crystalline domains, the strong interfacial tension of the liquid crystalline phase reduces the curvature of the branched domains and smoothes the protuberances on the surfaces of the domains. Because of the strong interfacial tension, the branched and continuously connected domains with small protuberances change to long and curved domains with flat surfaces, as shown in Fig. 2(f). Finally, the co-continuous structure shown in Fig. 1 is obtained.

To better understand the evolution of the co-continuous structure in Figs. 1 and 2, it is convenient to employ the integrated scattering intensity in $H\nu$ mode, i.e. the invariant $Q_{H\nu}$ defined by [23,32,33]

$$Q_{H\nu} = \int_0^\infty I(q) q^2 \mathrm{d}q \quad (3)$$

where I is the intensity of scattered light at the scattering vector q, $q=(4\pi/\lambda)\sin(\theta/2)$, λ and θ being the wavelength of the light and the scattering angle, respectively.

The $H\nu$ light scattering pattern from the liquid crystalline phase of BB-5 has a circular symmetric one, suggesting scattering from a liquid crystalline domain with randomly orientated optical anisotropy. In this case, $Q_{H\nu}$ is expressed by the mean square optical anisotropy $\langle\delta\rangle^2$

$$Q_{H\nu} \propto \langle\delta\rangle^2 = \phi_s(\alpha_r - \alpha_t)^2 \quad (4)$$

where ϕ_s is the volume fraction of the liquid crystalline domain, and α_r and α_t are the radial and tangential polarizabilities of the liquid crystalline domain,

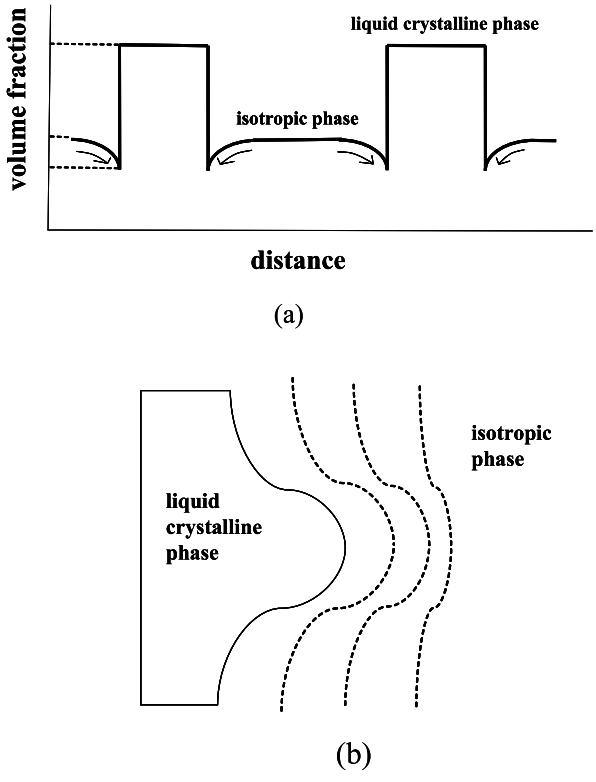

Fig. 3. Segregation of non-liquid crystallizable molecules from the growth front; (a) concentration gradient in front of the interface, (b) isothermal distribution in the isotropic melt region around the interface.

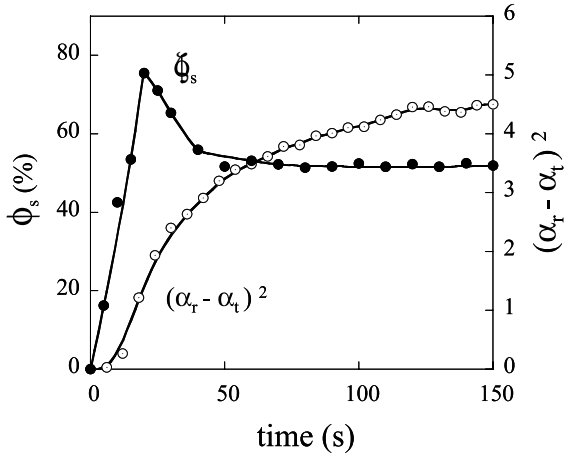

Fig. 4. Optical anisotropy and volume fraction of liquid crystalline phase in BB-5(WD) at 195 °C.

respectively. Therefore, Q_{Hv} is expected to increase with an increase in the volume fraction of the domain and then level off when the liquid crystallization stops [23,32,33].

During the evolution of the liquid crystallization at 180 °C, Q_{Hv} increased steeply at first, then increased gradually over time. This behavior indicates that liquid crystallization starts to occur after a short induction period and it stops after around 100 s. The volume fraction of the liquid crystalline domain ϕ_s was obtained by image data processing of particle analysis of the morphology shown in Fig. 2. The optical anisotropy $(\alpha_r - \alpha_t)^2$ is a measure of the ordering in the liquid crystalline domain. The value of $(\alpha_r - \alpha_t)^2$ can be obtained from Eq. (4) by Q_{Hv} and ϕ_s. Fig. 4 shows ϕ_s and $(\alpha_r - \alpha_t)^2$ thus obtained as a function of liquid crystallization time. ϕ_s increases steeply with time, and reaches a maximum at around 20 s, then starts to decrease. In contrast, $(\alpha_r - \alpha_t)^2$ increases steeply with time for the first 50 s, then continues to gradually increase with time. These results suggest that the liquid crystalline domain grows rapidly at an early stage with an increase in the ordering of the domain. The growth of the liquid crystalline domain stops after around 20 s. This corresponds with the result shown in Fig. 2(e). The decrease of ϕ_s suggests the contraction of the domain. The contraction may be ascribed to the reduction in surface area by interfacial tension and densification due to an increase of ordering after the liquid crystalline domain stops growing.

Fig. 5 shows optical micrographs of BB-5(WD) obtained by liquid crystallization at 185 and 193 °C. As the temperature of liquid crystallization increased, the rate of growth of liquid crystallization decreased and the liquid crystallizable region became narrower. Since the liquid crystallizable high molecular weight molecules decreased with increasing temperature, as demonstrated before, the liquid crystallizable region became narrower and the growth rate decreased with an increase in the liquid crystalline temperature. Distorted domains with small protuberances coalesced and branched domains were obtained at 185 °C (Fig. 5(a)). The sizes of the protuberances decreased and the domain became flatter with an increase in the liquid crystalline temperature, and multifaceted domains were obtained at a temperature of 193 °C (Fig. 5(b)). Since the contribution of supersaturation in Eq. (1) becomes smaller while that of the interfacial tension remains constant with an increase in temperature, the contribution of interfacial tension on interfacial stability in Eq. (1) becomes larger than that of supersaturation with an increase in temperature. Thus, distortion and branching decrease with an increase in temperature, and the interfaces become flatter by the suppression of the protuberances due to interfacial tension. This behavior may support the instability of the diffusion-controlled interface developed by the fractionation of the molecular weight distribution.

Fig. 6 shows the change in the morphology of BB-5(WD) during heating from 180 °C. During heating, the liquid crystalline region melted from the surface and became smaller. As shown in Fig. 7, the volume fraction of the liquid crystalline region continuously decreases with an increase in temperature. The volume fraction decreases gradually with an increase in temperature in BB-5(WD), while it decreases steeply in BB-5(ND). Since the smectic–isotropic phase transition temperature, T_i, increases with an increase in molecular weight and the liquid crystalline phase melts when it reaches T_i, continuous melting with temperature may be ascribed to the distribution of T_i due to the molecular weight distribution in the liquid crystalline phase. Therefore, T_i in BB-5 widens and the change in the

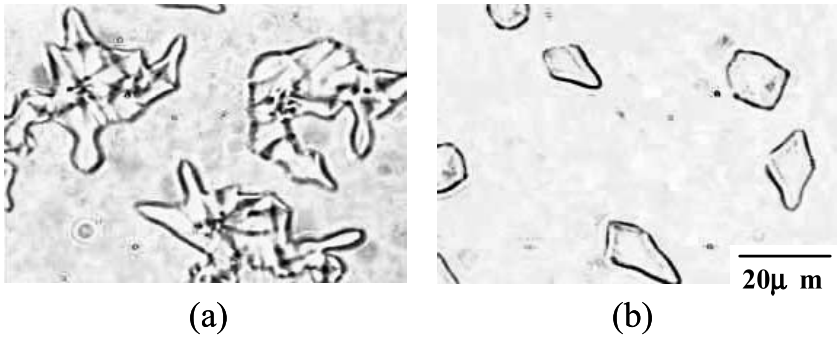

Fig. 5. Digital high-fidelity micrographs of BB-5(WD) at (a) 185 °C and at (b) 190 °C.

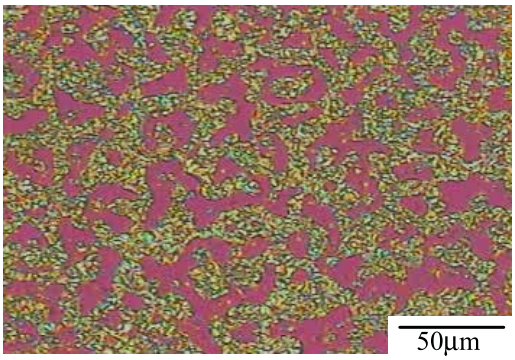

(a) 182 °C

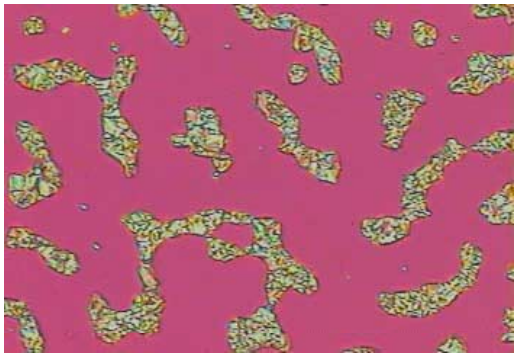

(b) 187 °C

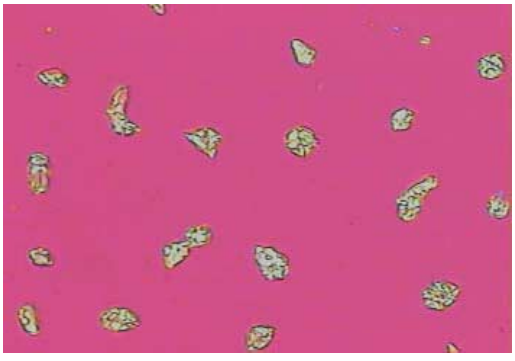

(c) 192 °C

Fig. 6. Polarized micrographs of BB-5(WD) during heating.

volume fraction becomes smaller as the molecular weight distribution increases. This behavior may also support the obtaining of the two-phase structure by the fractionation of the molecular weight distribution.

4. Conclusion

We found a co-continuous two-phase structure of a liquid crystalline phase and an isotropic phase in liquid crystalline polyester BB-5. The co-continuous structure is obtained by the coalescence and impingement of branched and distorted domains caused by fractionation of high and low molecular

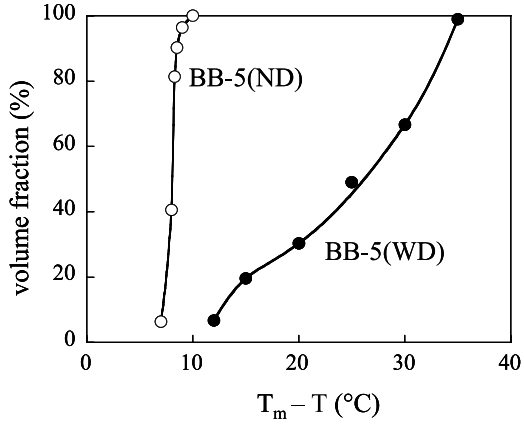

Fig. 7. Volume fraction of liquid crystalline region in BB-5(WD) and BB-5(ND) as a function of temperature during heating.

weight molecules during liquid crystallization. That is, a concentration gradient is formed at the growth front, and the growth front is unstable due to the segregation of the non-liquid crystallizable low molecular weight molecules. Such structure development is quite different from the morphology development by liquid–liquid phase separation via spinodal decomposition, and it may be attributed to the segregation of non-liquid crystallizable low molecular weight molecules from the growth front by fractionation of the molecular weight distribution during the liquid crystallization.

References

[1] Imai M, Mori K, Mizukami T, Kaji K, Kanaya T. Polymer 1992;33:4451.
[2] Imai M, Kaji K, Kanaya T. Macromolecules 1994;27:7103.
[3] Ezquerra TA, López-Cabarcos E, Hsiao BS, Baltá-Calleaja FJ. Phys Rev E 1996;54:989.
[4] Terrill NJ, Fairclough PA, Towns-Andrew E, Komanschek BU, Young RJ, Ryan AJ. Polymer 1998;39:2381.
[5] Heeley EL, Maidens AV, Olmsted PD, Bras W, Dolbnya IP, Fairclough JPA, et al. Macromolecules 2003;36:3656.
[6] Matsuba G, Kaji K, Nishida K, Kanaya T, Imai M. Macromolecules 1999;32:8932.
[7] Olmsted PD, Poon WCK, McLeish TCB, Terrill NJ, Ryan AJ. Phys Rev Lett 1998;81:373.
[8] Doi M, Shimada T, Okano K. J Chem Phys 1988;88:4070.
[9] Wang W, Shiwaku T, Hashimoto T. Macromolecules 2003;36:8088.
[10] Suzuki K, Saito H, Tokita M, Watanabe J. Polym Prepr Jpn 2002;51:560.
[11] Mullins WW, Sekerka RF. J Appl Phys 1963;34:323.
[12] Keith HD, Padden Jr FJ. J Appl Phys 1963;34:2409.
[13] Keith HD, Padden Jr FJ. Polymer 1986;27:1463.
[14] Cahn JW. In: Peiser HS, editor. Crystal growth. New York: Pergamon; 1967. p. 681.
[15] Langer JS. Rev Mod Phys 1980;52:1.
[16] Goldenfeld N. J Cryst Growth 1987;84:601.
[17] Saito Y. Statistical physics of crystal growth. London: World Scientific Publishing; 1996.
[18] Watanabe J, Hayashi M. Macromolecules 1988;21:278.
[19] Watanabe J, Hayashi M. Macromolecules 1989;22:4083.
[20] Watanabe J, Hayashi M, Nakata Y, Niori T, Tokita M. Prog Polym Sci 1997;22:1053.

[21] Watanabe J, Kinoshita S. J Phys (France) 1992;2:1273.
[22] Tokita M, Osada K, Watanabe J. Polym J 1998;30:589.
[23] Lee CH, Saito H, Inoue T. Macromolecules 1993;26:6566.
[24] Toh KC, Wang W. Macromolecules 2000;33:2055.
[25] Wang W, Hashimoto T. Polymer 2000;41:4729.
[26] Lester CL, Guymon CA. Polymer 2002;43:3707.
[27] Banach MJ, Friend RH, Sirringhaus H. Macromolecules 2003;36:2838.
[28] Collyer AA, editor. Liquid crystal polymers: From structure to applications. London: Elsevier Applied Science; 1992.
[29] Dierking I. Textures of liquid crystals. Weinheim: Wiley-VCH; 2003.
[30] Keith HD, Padden Jr FJ. J Appl Phys 1964;35:1286.
[31] Taguchi K, Miyaji H, Izumi K, Hoshino A, Miyamoto Y, Kokawa R. Polymer 2001;42:7443.
[32] Koberstein J, Russell TP, Stein RS. J Polym Sci, Polym Phys Ed 1979; 17:1719.
[33] Tsuburaya M, Saito H. Polylmer 2004;45:1027.